Cancer Cell International

RESEARCH

Open Access

Celastrol attenuates the invasion and migration and augments the anticancer effects of olaparib in prostate cancer

Mengqiu Huang[1], Lin Chen[4], Xiaoyan Ma[5] and Houqiang Xu[1,2,3,6*]

Abstract

Background Prostate cancer (PCa) is a leading malignancy among men globally, with rising incidence rates emphasizing the critical need for better detection and therapeutic approaches. The roles of HSP90AB1 and PARP1 in prostate cancer cells suggest potential targets for enhancing treatment efficacy.

Methods This study investigated the overexpression of HSP90AB1 and PARP1 in prostate cancer cells and the impact of HSP90AB1 knockdown on the sensitivity of these cells to the PARP inhibitor olaparib. We also explored the combined effect of olaparib and celastrol, an HSP90 inhibitor, on the clonogenic survival, migration, proliferation, and overall viability of prostate cancer cells, alongside the modulation of the PI3K/AKT pathway. An in vivo PC3 xenograft mouse model was used to assess the antitumor effects of the combined treatment.

Results Our findings revealed significant overexpression of HSP90AB1 and PARP1 in prostate cancer cells. Knockdown of HSP90AB1 increased cell sensitivity to olaparib. The combination of olaparib and celastrol significantly reduced prostate cancer cell survival, migration, proliferation, and enhanced cumulative DNA damage. Celastrol also downregulated the PI3K/AKT pathway, increasing cell susceptibility to olaparib. In vivo experiments demonstrated that celastrol and olaparib together exerted strong antitumor effects.

Conclusions The study indicates that targeting both HSP90AB1 and PARP1 presents a promising therapeutic strategy for prostate cancer. The synergistic combination of celastrol and olaparib enhances the efficacy of treatment against prostate cancer, offering a potent approach to combat this disease.

Keywords Prostate Cancer, HSP90AB1, PARP1, Olaparib, Celastrol, PI3K/AKT pathway

*Correspondence:
Houqiang Xu
gzdxxhq@163.com
[1]College of Biology and Environmental Engineering, Guiyang University, Guiyang, Guizhou, China 550005
[2]Key Laboratory of Animal Genetics, Breeding and Reproduction in the Plateau Mountainous Region, Ministry of Education, Guizhou University, Guiyang, Guizhou, China
[3]College of Animal Science, Guizhou University, Guiyang, Guizhou, China
[4]Department of Ophthalmology, Affiliated Hospital of Zunyi Medical University, Zunyi, Guizhou, China
[5]College of Food and Pharmaceutical Engineering, Guizhou Institute of Technology, Guiyang, Guizhou, China
[6]Department of Biomedicine, Guizhou University school of Medicine, 2708#, Huaxi Road South, Huaxi District, Guiyang 550025, Guizhou, China

Background

Prostate cancer (PCa) is one of the most prevalent malignancies affecting men globally, marked by its heterogeneous nature and variable clinical outcomes [1, 2]. It ranges from indolent tumors, which may need minimal to no treatment, to aggressive forms that require prompt and often multifaceted therapeutic strategies [3]. The development of PCa is influenced by a complex interplay of genetic, environmental, and lifestyle factors [4, 5]. Despite advances in early detection and treatment, PCa remains a significant public health challenge [6]. Early detection through screening, such as PSA (Prostate-Specific Antigen) testing, has been pivotal in identifying potential cases, yet it raises concerns regarding overdiagnosis and overtreatment [1, 7]. Androgen deprivation therapy (ADT) is crucial in treating PCa, primarily by reducing androgen levels to inhibit tumor growth [8]. However, its effectiveness diminishes over time with the development of castration-resistant prostate cancer (CRPC), and prolonged use leads to significant side effects like osteoporosis and cardiovascular issues [9]. Specific drugs like abiraterone, enzalutamide, docetaxel, and sipuleucel-T have shown efficacy, particularly in advanced stages. Abiraterone and enzalutamide target the androgen receptor pathway, while docetaxel is a chemotherapy agent, and sipuleucel-T is an immunotherapy [10]. However, their limitations include the development of drug resistance, particularly in metastatic castration-resistant prostate cancer (mCRPC) [10, 11]. Recent trends in research and treatment have focused on personalized medicine approaches, integrating patient-specific genetic and molecular profiles to guide therapy. As the demographic shifts towards an older population, the incidence and impact of PCa are expected to rise, underscoring the need for continued research and innovation in its management.

HSP90AB1 (heat shock protein 90 kDa alpha, class B, member 1), a member of the HSP90 (heat shock protein 90) family, plays a pivotal role in cellular homeostasis and protein folding. As a molecular chaperone, it assists in the proper folding and functional maintenance of various client proteins, including kinases, hormone receptors, and transcription factors [12]. Elevated expression of HSP90AB1 has been observed across various solid tumors, indicating its significant role in oncogenesis. Multiple investigations have revealed that HSP90AB1 facilitates tumorigenesis in a spectrum of cancers, including gastric cancer, breast cancer, non-small cell lung cancer (NSCLC), hepatocellular carcinoma, and head and neck squamous cell carcinoma [13–18]. It supports the stability and function of numerous oncoproteins, thereby facilitating tumor growth, survival, and resistance to therapies [19, 20]. The involvement of HSP90AB1 in these processes makes it a potential target for cancer therapeutics, with research increasingly focusing on HSP90 inhibitors to disrupt its function in cancer cells.

Celastrol, a pentacyclic triterpenoid extracted from *Tripterygium wilfordii* roots, selectively destabilizes steroid receptors by inhibiting HSP90AB1 activity and altering the three-dimensional structure of its co-chaperone p23 [21]. Gaining prominence for its anti-inflammatory and antioxidant properties [22, 23], celastrol has recently emerged as a potential therapeutic agent in cancer treatment. Studies have also highlighted its role in enhancing the efficacy of existing chemotherapeutic agents, positioning celastrol as a promising adjunct in cancer therapy [24]. Owing to its ability to target critical molecular pathways and its prospective synergistic effects with other anticancer agents, the research potential of celastrol in cancer therapy is substantial.

PARP inhibitors, notably olaparib, have emerged as significant therapeutic agents, particularly in cancers with defective DNA repair mechanisms, such as BRCA-mutated tumors [25]. Olaparib, has shown substantial efficacy in various cancers, including ovarian, breast, and PCa [26–28]. Its mechanism of action involves the trapping of PARP on damaged DNA, leading to cell death, especially in cells deficient in homologous recombination repair (HRR) [29]. In PCa, olaparib has gained attention for its effectiveness in patients with mutations in DNA repair genes, offering a targeted treatment approach [28, 30]. However, resistance inevitably emerges during its clinical application, which can lead to cancer progression and reduced survival rates, posing a substantial challenge in clinical management [31]. The combination of olaparib with other therapeutic agents in cancer treatment holds significant clinical implications, offering a strategy to enhance efficacy and overcome resistance of monotherapy. When combined with drugs targeting other pathways, such as angiogenesis inhibitors, immune checkpoint blockers, or chemotherapy agents, can lead to synergistic effects [29]. Such combinational strategies are crucial for optimizing therapeutic outcomes and expanding the scope of effective treatments in oncology.

In this study, we discovered that both HSP90AB1 and PARP1 are significantly overexpressed in PCa cell lines, and the elevated expression levels of these proteins are associated with a lower overall survival probability in patients with PCa. Interference with HSP90AB1 expression enhanced the sensitivity of PCa cell lines to olaparib. Functional assays demonstrated that combination therapy with celastrol and olaparib had superior efficacy compared to monotherapy in both in vitro and in vivo models. This study underscores the potential of using a combination of celastrol and olaparib as an innovative therapeutic approach for PCa.

Methods

Data resources

The expression and transcript data for HSP90AB1 and PARP1 were obtained from TCGA projects. Kaplan-Meier curves representing survival of PCa patients with different expression of HSP90AB1 or PARP1 as determined using the publicly available R2 platform (r2.amc.nl). The Correlation Analysis between HSP90AB1 and PARP1 was plotted by freely accessible GEPIA Database (http://gepia2.cancer-pku.cn/).

Cell culture and drugs

The cell lines RWPE-1, 22RV1, PC3, and DU145 were procured from Zhong Qiao Xin Zhou Biotechnology Co., Ltd., Shanghai, China. The RWPE-1 cells were propagated in a specialized medium provided by ZQXZ Bio, Shanghai, China. Both 22RV1 and DU145 cell lines were maintained in RPMI-1640 medium, enriched with 10% fetal bovine serum (FBS) and 1% penicillin-streptomycin (P/S), and incubated at 37 °C within an atmosphere containing 5% CO2. Similarly, PC3 cells were grown in F-12 K medium formulated by ATCC, supplemented with 10% FBS and 1% P/S, and also incubated at 37 °C in a 5% CO_2 ambiance. The pharmacological agents olaparib (AZD2281) and celastrol (HY-13067) were sourced from MedChemExpress, Monmouth Junction, NJ, USA.

Antibodies

Antibodies against HSP90AB1 (11405-1-AP) and GAPDH (60004-1-Ig) were obtained from Proteintech (Wuhan, China). Antibodies against PARP1 (ab227244), γH2AX (phospho S139) (ab81299) and Ki-67 (ab92742) were purchased from Abcam (Cambridge, UK). Antibodies against p-AKT (phospho Ser473) (4060T), AKT (4691T), p-PI3K (phospho Tyr458/Tyr199) (17366s) and PI3K (4257T) were purchased from Cell Signaling Technology (Beverly, MA, USA).

Plasmids and short hairpin RNA transfection

The interference plasmid for HSP90AB1 and the negative control plasmid shNC are preserved in our laboratory. Transfection of all plasmids was performed using FuGENE®HD transfection reagent (Promega Corporation, Madison, WI, USA).

Western blot analysis

Cells were harvested and lysed using RIPA buffer for protein extraction. Protein concentrations of the lysates were quantified utilizing the bicinchoninic acid (BCA) assay. Equivalent amounts of protein from each lysate were combined with SDS sample buffer, subjected to SDS-PAGE, and electrotransferred onto polyvinylidene fluoride (PVDF) membranes. The membranes were blocked in nonfat dry milk for 2 h at 37 °C, followed by overnight incubation at 4 °C with primary antibodies. Subsequent incubation with the corresponding secondary antibodies was conducted at a dilution of 1:10,000 for 1 h at 37 °C. The membranes were then washed with TBST and developed using an enhanced chemiluminescence (ECL) detection system.

Cell viability and colony formation assay

Cell viability was assessed using a Cell Counting Kit-8 (CCK-8) assay (APExBIO Technology LLC, Houston, USA) according to the manufacturer's instructions with minor modifications. Post-drug treatment or plasmid transfection, cells were plated at a density of around 5,000 cells per well into 96-well plates. At the 24 h, 48 h, and 72 h marks of incubation, the medium was supplemented with 10% CCK-8 and continued to incubate for a further 2 h. Cell viability was measured at 450 nm using a Multiskan Spectrum instrument (Synergy H4, BioTek, USA).

To assess the colony-forming capability of cells after treatment, a colony formation assay was performed. Cells were first treated with different drugs. Following trypsinization and cell counting, 22RV1 cells were seeded at 800 cells per well, while PC3 and DU145 cells were seeded at 500 cells per well, in 6-well plates. Cells were cultured at 37 °C in a humidified atmosphere with 5% CO2. The medium was refreshed every 3 to 4 days to provide nutrients essential for colony growth. After an incubation for 2 weeks, the cells were washed gently with phosphate-buffered saline (PBS) and fixed with 4% paraformaldehyde for 15 min at room temperature. Fixed colonies were stained with 0.5% crystal violet in 20% methanol for 15 min to enhance visibility. Excess stain was washed away with tap water, and plates were air-dried. The number of colonies was counted using ImageJ 1.8.0 software (National Institutes of Health, Bethesda, MD, USA).

Wound scratch assay

The wound scratch assay was conducted to evaluate cell migration. Cells were seeded in 6-well plates and grown to 90–100% confluence to form a monolayer. After reaching confluence, the monolayer was scratched with a sterile 10 μL pipette tip to create a straight-line "wound". Debris was removed by washing the cells gently with PBS. Subsequently, the cells were incubated in medium with reduced serum and drug.

Photographs of the scratch were taken immediately after the wound was made (0 h), recorded as w1. The same area of the scratch was photographed at subsequent time points (e.g., 48 h, recorded as w2) to monitor cell migration into the wound space. The relative migration rate was calculated using the formula: (w1 - w2) / w1×100%.

EdU assay

Cell proliferation was assessed using an EdU assay, which is based on the incorporation of the thymidine analog 5-ethynyl-2'-deoxyuridine (EdU) into DNA during active DNA synthesis. This assay was conducted using the EdU imaging kits (APExBIO Technology LLC, Houston, USA). Briefly, cells were seeded in 6-well plates and allowed to attach overnight. Following treatment with different drugs, cells were incubated with EdU (10 μM) for 2 h to label proliferating cells. After EdU incubation, cells were fixed with 4% paraformaldehyde for 15 min at room temperature and permeabilized with 0.5% Triton X-100 in PBS for 20 min. After the click-it reaction was performed, fluorescent microscopy was used to visualize and quantify the incorporated EdU (indicative of DNA synthesis) and DAPI (indicating total cell nuclei). The percentage of EdU-positive cells was calculated by counting the number of EdU-stained cells and dividing by the total number of DAPI-stained cells, multiplying by 100.

Immunofluorescence (IF) and immunohistochemistry (IHC) assay

Cells were seeded on coverslips placed in culture dishes and grown to the desired confluence. After treatment, cells were fixed with 4% paraformaldehyde for 15 min at room temperature and then permeabilized with 0.1% Triton X-100 in PBS for 10 min. Non-specific binding was blocked by incubating cells in blocking buffer (5% bovine serum albumin in PBS) for 1 h at room temperature. Cells were then incubated with primary antibody overnight at 4 °C. After washing with PBS, cells were incubated with fluorochrome-conjugated secondary antibodies for 1 h at room temperature in the dark. Nuclei were stained with DAPI for 5 min. Coverslips were mounted onto glass slides using an anti-fade mounting medium. The IF images were captured using an Olympus IX71 Nikon imaging system.

For IHC staining, tissue sections were deparaffinized in xylene and rehydrated through a graded alcohol series. Antigen retrieval was performed by heating the slides in a citrate buffer (pH 6.0) in a microwave. Endogenous peroxidase activity was quenched with 3% hydrogen peroxide for 10 min. Non-specific binding was blocked by incubating the sections in blocking solution (5% normal serum) for 1 h at room temperature. Sections were then incubated with primary antibodies overnight at 4 °C. After washing, the sections were incubated with biotinylated secondary antibodies, followed by further incubation with an avidin-biotin-peroxidase complex. The signal was developed using a DAB (3,3'-diaminobenzidine) substrate kit, resulting in a brown coloration at the antigen site. The sections were counterstained with hematoxylin, dehydrated, and mounted. The stained sections were examined under a light microscope, and images were captured for analysis.

Alkaline comet assay

Cells were harvested and resuspended in PBS at a concentration of 1×10^6 cells/mL. The cell suspension was then mixed with 0.75% low melting point agarose at a ratio of 1:10 (v/v) and immediately pipetted onto a frosted microscope slide pre-coated with 1% normal melting point agarose. The slides were covered with coverslips and left at 4 °C for 10 min to solidify the agarose. Once solidified, coverslips were gently removed, and the slides were submerged in a lysis buffer (2.5 M NaCl, 100 mM EDTA, 10 mM Tris, with 1% Triton X-100 and 10% DMSO, pH 10) at 4 °C for 1 h to lyse the cells and allow DNA unfolding. Following lysis, the slides were placed in an electrophoresis buffer (300 mM NaOH, 1 mM EDTA, pH>13) for 20 min to allow DNA unwinding and the expression of alkali-labile sites. Electrophoresis was conducted at 25 V and 300 mA (1 V/cm) for 30 min. Post electrophoresis, the slides were neutralized with 0.4 M Tris buffer (pH 7.5) for 5 min and then stained with ethidium bromide (20 μg/mL). The slides were photographed for analysis under a fluorescence microscope. Images of the comets were captured and subsequently analyzed using appropriate image analysis software to quantify DNA damage.

In vivo xenograft studies

Male BALB/c nude mice, 5–6 weeks old, were procured from SJA Laboratory Animal Co., Ltd., Changsha, China. These mice underwent a quarantine period of one week before any experimental procedures. Tumor xenografts were established by subcutaneously injecting 1 million (1×10^6) PC3 cells, suspended in 100 μL PBS, into the right flank of each mouse. Subsequently, the mice were randomly allocated into various groups, with each group comprising 6 mice. Treatment groups were administered intraperitoneal injections of celastrol (2 mg/kg) and olaparib (30 mg/kg), either as monotherapies or in combination, thrice weekly for a total of 3 weeks. Tumor sizes were measured and recorded every 3 days, calculating tumor volume with the formula: (length × width^2)/2. All procedures involving animals were performed in compliance with the ethical guidelines and approval of the Laboratory Animal Ethics Committee at Guizhou University.

Statistical analysis

Data are expressed as mean±standard deviation (SD), derived from at least three separate experiments. Statistical differences between two groups were evaluated using the Student's two-tailed t-test. For comparisons across multiple groups, one-way ANOVA was employed. All statistical analyses were performed using GraphPad Prism version 8.0 software. Significance levels were set as

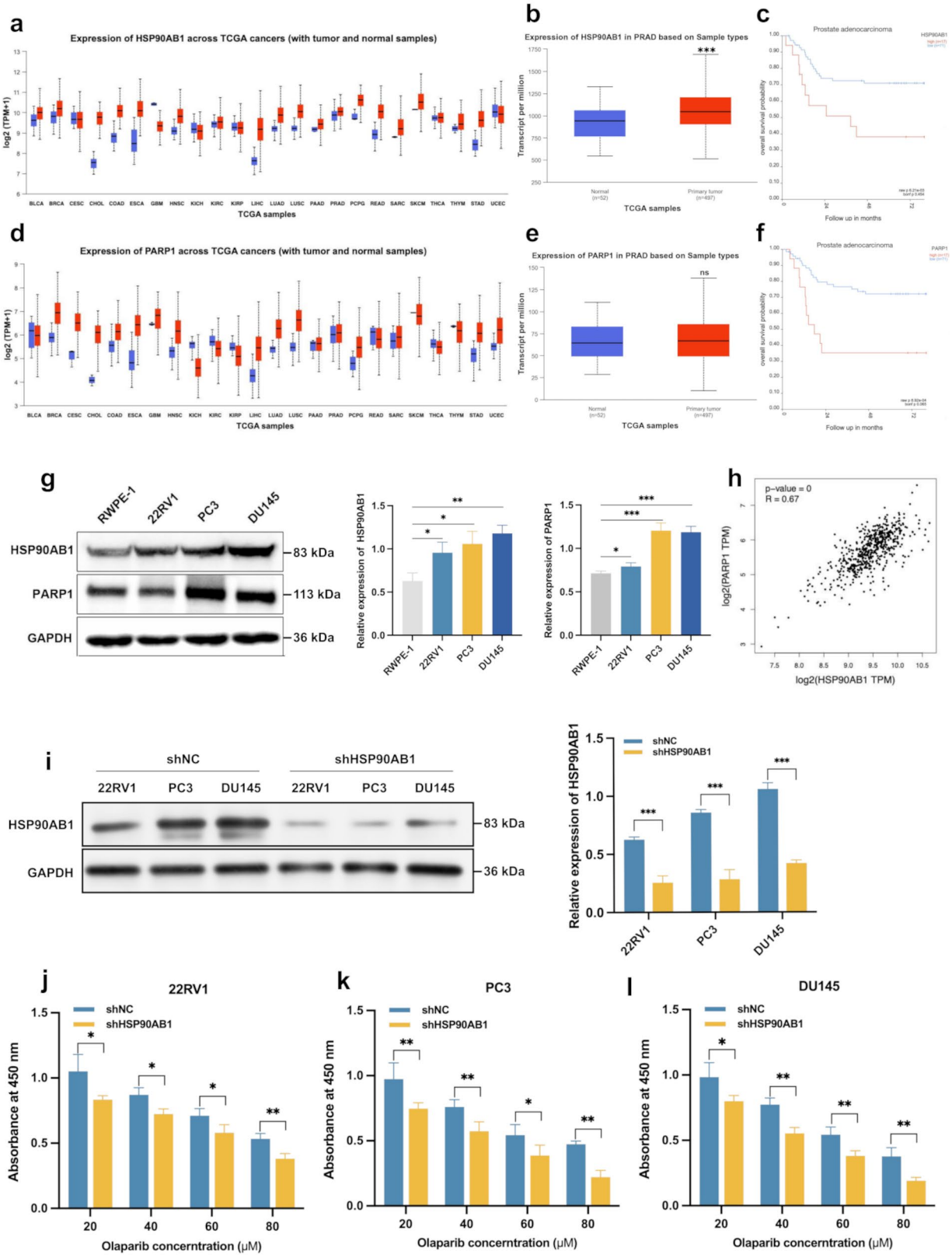

Fig. 1 (See legend on next page.)

(See figure on previous page.)

Fig. 1 HSP90AB1 and PARP1 expression is elevated in PCa, and HSP90AB1 silencing increases olaparib sensitivity in PCa cell lines. (**a**) Differential expression of HSP90AB1 across various cancer types as compared to normal tissue samples in the Cancer Genome Atlas (TCGA) Database. (**b**) The transcript levels of the HSP90AB1 in PRAD were acquired from the TCGA database. (**c**) Elevated HSP90AB1 expression correlated with a diminished overall survival probability among patients with PCa. (**d**) Expression of PARP1 in various cancers versus normal tissues from TCGA. (**e**) The transcript levels of the PARP1 in PRAD were acquired from the TCGA database. (**f**) High expression of PARP1 was associated with poor overall survival probability in PCa patients. (**g**) Western blot analysis of HSP90AB1 and PARP1 protein levels in PCa cell lines. (**h**) Correlation of HSP90AB1 and PARP1 gene expression in PCa samples. The dataset came from GEPIA (http://gepia.cancer-pku.cn/). (**i**) Knockdown efficiency of HSP90AB1 in PCa cell lines. (**j-l**) Sensitivity of PCa cell lines to different concentration of olaparib (20, 40, 60, 80 μM) following HSP90AB1 knockdown. Shown are the means ± SD from 3 experiments (*$P < 0.05$, **$P < 0.01$, ***$P < 0.001$)

follows: *$P<0.05$, **$P<0.01$, ***$P<0.001$, with "ns" indicating a lack of significant difference. A P-value less than 0.05 was considered to denote statistical significance.

Results

The expression of HSP90AB1 and PARP1 are significantly higher in PCa and HSP90AB1 knockdown enhanced the sensitivity of PCa cell lines to olaparib

To assess HSP90AB1 and PARP1 expression in PCa, we queried the TCGA database. Fig. 1a and d illustrate the expression levels of HSP90AB1 and PARP1, respectively, across different TCGA cancer cohorts, with both tumor and adjacent normal samples. The data indicated higher expression levels of these genes in tumor samples compared to normal tissues. Specifically focusing on prostate adenocarcinoma (PRAD), Fig. 1b revealed that HSP90AB1 transcripts are significantly elevated in primary tumor tissues compared to normal samples. Similarly, Fig. 1e demonstrated an upregulation of PARP1 expression in PRAD tumor samples versus normal counterparts. Furthermore, our investigation employed the R2 platform (r2.amc.nl), which encompasses gene expression profiles from extensive patient cohorts and provides analytical tools for comparing gene expression across various cancer types. The findings revealed a correlation between heightened expression of HSP90AB1 and PARP1 and diminished overall survival in patients with PRAD, as illustrated in Fig. 1c and f.

To confirm the upregulation of HSP90AB1 and PARP1 in PCa, we conducted western blot assays on three human PCa cell lines (22RV1, PC3, and DU145) alongside normal human prostate cells (RWPE-1). In alignment with prior observations, protein levels of HSP90AB1 and PARP1 were found to be higher in the PCa cell lines relative to the normal control (Fig. 1g). Moreover, using the GEPIA platform to examine the TCGA dataset for PRAD, we observed a significant positive correlation between the expression of PARP1 and HSP90AB1 proteins (Fig. 1h).

To assess the influence of HSP90AB1 in mediating the anti-tumor sensitivity to olaparib, we utilized shRNA to knockdown HSP90AB1 and then examined the viability of PCa cell lines (22RV1, PC3, and DU145) in the presence of olaparib. Western blot analysis was employed to evaluate the silencing efficiency of HSP90AB1 in three human PCa cell lines compared to a non-targeting control shNC. The results demonstrated a significant reduction in HSP90AB1 expression in the shHSP90AB1 groups across all three cancer cell lines (Fig. 1i). Furthermore, CCK-8 assays following treatment with varying concentrations of olaparib (20, 40, 60, 80 μM) revealed that HSP90AB1 knockdown significantly enhanced the sensitivity of these PCa cell lines to olaparib (Fig. 1j-l). These results indicated that both PARP1 and HSP90AB1 are significantly overexpressed in PCa, and suppression of HSP90AB1 effectively enhances the sensitivity of PCa cell lines to olaparib in a dose-dependent manner.

The combination of olaparib and celastrol was observed to more effectively attenuate clonogenicity, migration, proliferation, and overall viability in PCa cells

Celastrol, a triterpenoid derivative, has been shown to impede the activity of HSP90AB1 [21]. Given that HSP90AB1 knockdown augments the sensitivity of PCa cells to olaparib, we posited that celastrol may potentiate the efficacy of olaparib in these cells. Colony formation assays indicated that the co-administration of celastrol and olaparib significantly reduced the clonogenic capacity of PCa cells more effectively than either agent alone (Fig. 2a). Similarly, wound healing assays demonstrated that the combination therapy markedly inhibited the migration of PCa cells compared to monotherapy (Fig. 2b, c). Due to the difficulty in forming a monolayer with 22RV1 cells, which could potentially affect the experimental outcomes, this cell line was not utilized in subsequent phenotypic experiments.

To further validate the impact of combination therapy on the proliferation and viability of PCa cells, we conducted both EdU incorporation and CCK-8 assays. The results demonstrated that the combined treatment significantly inhibited the proliferation and viability of PC3 and DU145 cells compared to the monotherapy groups (Fig. 2d and f). These findings indicated that celastrol amplifies the antitumor activity of olaparib, suggesting that the combined use of celastrol and olaparib exerts a superior inhibitory effect on PCa cells.

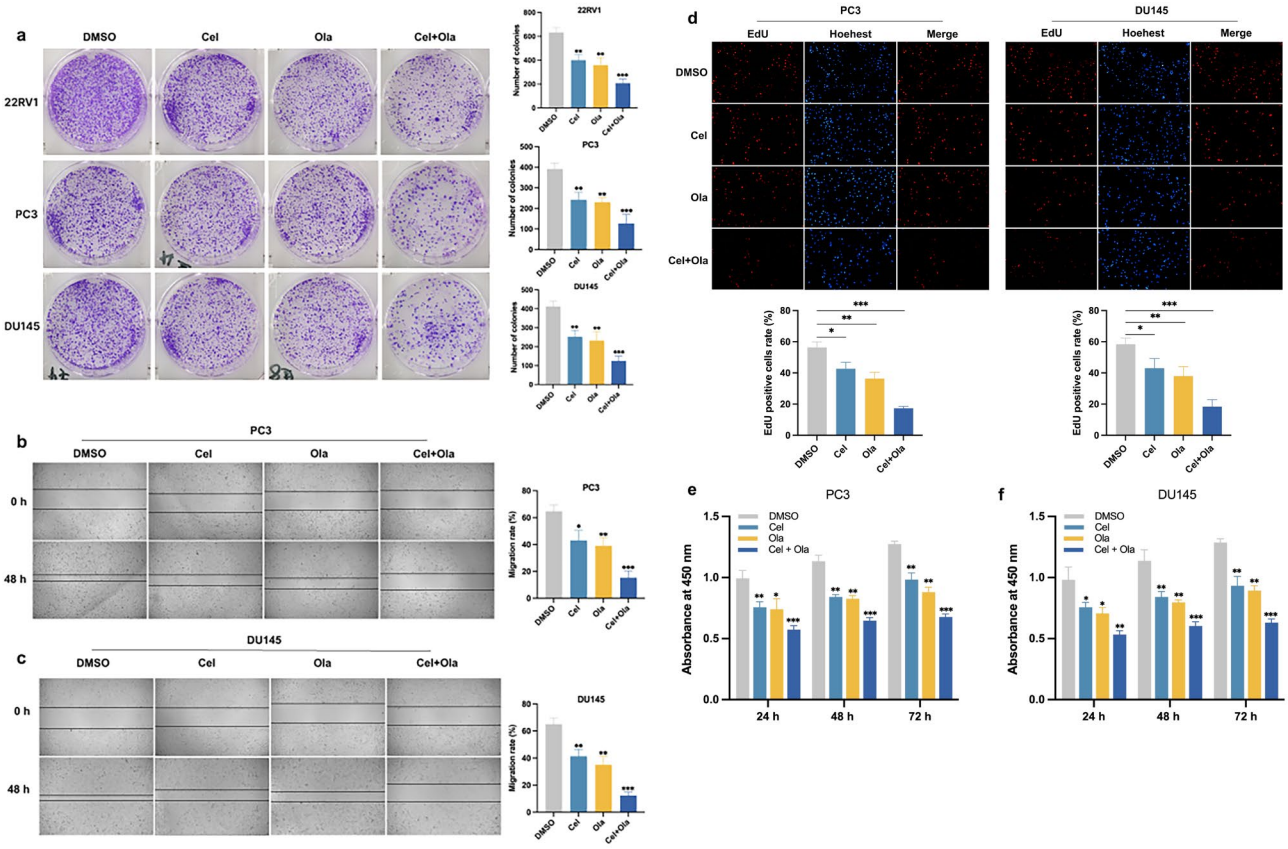

Fig. 2 The olaparib-celastrol combination more effectively impairs clonogenicity, migration, and growth of PCa cells. (**a** Colony formation assay of 22RV1, PC3, and DU145 cell lines following treatment with celastrol (1 μM) and olaparib (50 μM) or monotherapy, or DMSO. (**b-c**) Wound scratch assay of PC3 and DU145 cell lines treated with celastrol (1 μM) and olaparib (50 μM) or monotherapy, or DMSO. Scale bars: 500 μm. (**d-e**) Evaluation of proliferation and viability in PC3 and DU145 cell lines subjected to treatments with DMSO, celastrol (1 μM), olaparib (50 μM), and their combination through EdU and CCK-8 assays. Scale bars: 50 μm. Shown are the means ± SD from 3 experiments (*$P < 0.05$, **$P < 0.01$, ***$P < 0.001$)

Olaparib and celastrol augment cumulative DNA damage in PCa cells

Double-strand breaks (DSBs) are potent instigators of mutagenesis and cellular demise, representing the most deleterious type of DNA damage. In metazoans, a singular DSB has the potential to be lethal if it remains unrepaired [32]. Phosphorylated histone H2AX (γH2AX) serves as a biomarker for cellular responses to DSBs, with implications for tracking DNA damage and repair in human populations [33]. To assess the effects of celastrol and olaparib on DSBs, we measured the formation of γH2AX foci in PCa cells. The results indicated that the combination treatment group with celastrol and olaparib significantly increased the formation of γH2AX foci compared to the monotherapy groups in PCa cells (Fig. 3a). Similarly, western blot results also revealed a significant upregulation of γH2AX expression in the combination treatment group (Fig. 3b).

Upon observing that celastrol as single-agent elevated γH2AX levels in PCa cells, we subsequently assessed whether the adjunctive application of the PARP inhibitor olaparib would further impair the cellular DNA damage response. Both celastrol and olaparib, when used as monotherapies, moderately increased DNA damage, as evidenced by tail moment assays. However, the concomitant administration of celastrol and olaparib markedly intensified DNA damage in PC3 and DU145 cells (Fig. 3c). These results suggest that celastrol and olaparib impede DSB repair in a sustained manner, thereby exerting a synergistic effect on antitumor activity.

Celastrol downregulates the PI3K/AKT pathway and enhances the susceptibility of PCa cells to olaparib

The PI3K/AKT signaling axis is critical in the tumorigenic process of PCa, influencing apoptosis, proliferation, metastasis, and invasion. It modulates various pathways integral to cellular growth, apoptosis, and invasive behavior. Consequently, PI3K/AKT represents a pivotal juncture in both the pathogenesis and treatment of PCa [34, 35]. To explore the functional impact of combination treatment on the PI3K/AKT pathway in PCa, we exposed PCa cells to celastrol, olaparib, or monotherapy for 48 h and subsequently assessed the expression of several proteins. Our results revealed that, relative to monotherapy

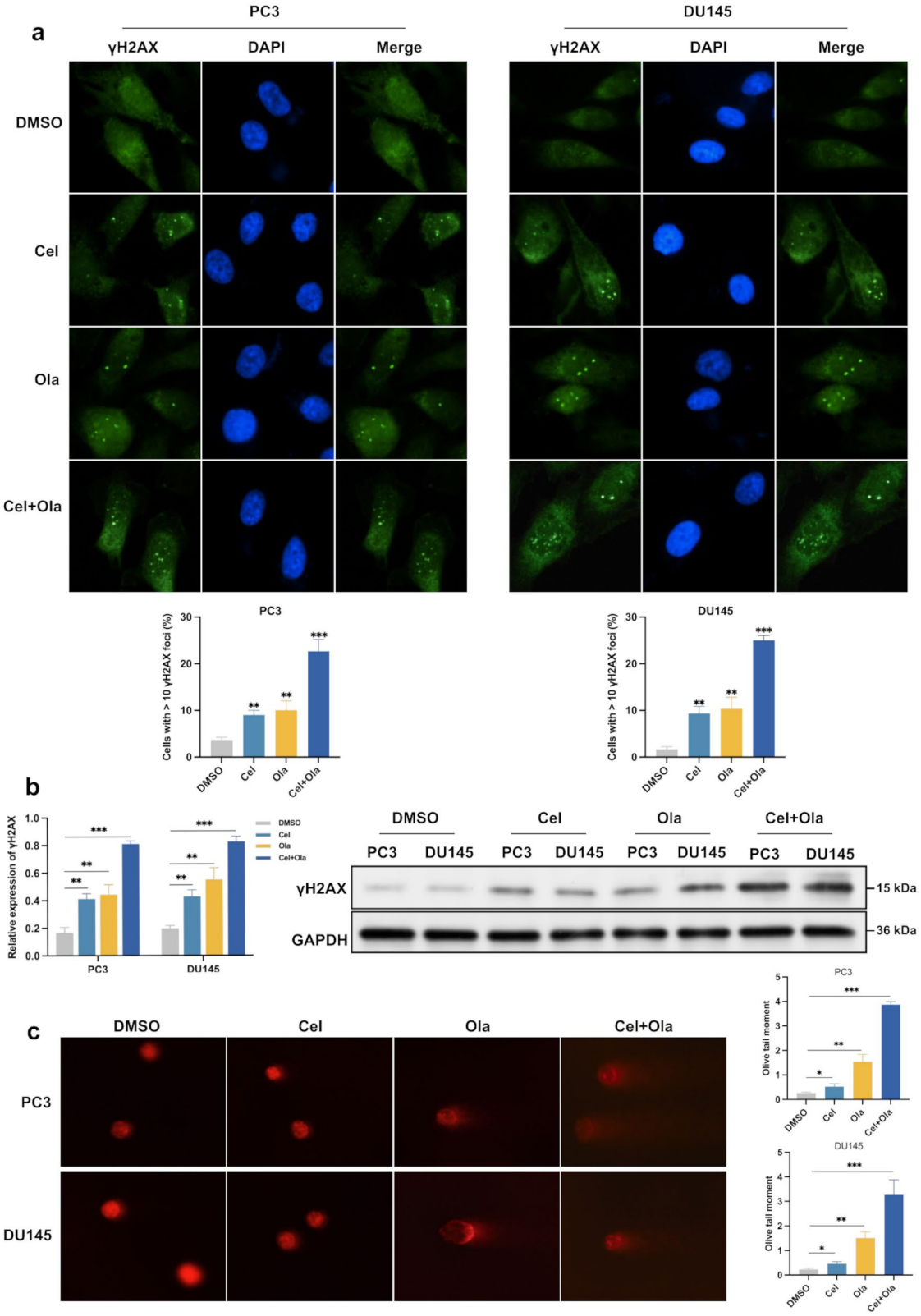

Fig. 3 Olaparib and celastrol enhanced total DNA damage in PCa cells. (**a**, **b**) IF staining and western blot demonstrated γH2AX expression in PCa cells following a 48 h treatment with celastrol (1 μM) and olaparib (50 μM), celastrol or olaparib monotherapy, or DMSO. Scale bars: 25 μm. (**c**) Comet assay of PC3 cells treated with celastrol (1 μM) and olaparib (50 μM), either agent alone, or DMSO, for 48 h. The olive tail moment served as the metric for analysis and underwent statistical evaluation. Scale bars: 20 μm. Shown are the means ± SD from 3 experiments (*$P < 0.05$, **$P < 0.01$, ***$P < 0.001$)

with olaparib, the concurrent administration of celastrol and olaparib further diminished the levels of phosphorylated AKT and PI3K proteins, which are downstream targets of the PI3K/AKT signaling pathway, in PC3, DU145, and 22RV1 cell lines as shown in Fig. 4. This suggests that while celastrol alone can reduce phosphorylated PI3K/AKT levels, the combination therapy may provide a more comprehensive inhibition of the pathway, potentially overcoming resistance mechanisms that could arise from monotherapy with olaparib. Furthermore, the combined treatment targets multiple aspects of the signaling cascade, enhancing therapeutic efficacy and reducing the likelihood of tumor resistance.

The anti-tumor effect of celastrol combined with olaparib on PC3 xenografts in vivo

To further validate the combined therapeutic efficacy of celastrol and olaparib in vivo, we conducted a xenograft tumor experiment. Nude mice bearing PC3-derived xenografts were administered DMSO, celastrol, olaparib, or a combination of celastrol and olaparib. On day 26, tumors were harvested, weighed, and processed for IHC staining (Fig. 5a). Tumor volume and weight were quantified to evaluate neoplastic progression. The results showed that relative to the DMSO control, combination therapy with celastrol and olaparib markedly diminished both tumor weight ($P<0.001$) and volume ($P<0.01$) in the PC3 xenograft model (Fig. 5b, c). To monitor for potential toxicity, body weight and the weights of major organs, including the liver, kidney, heart and spleen were measured. Regarding body weight, mice treated solely with celastrol showed a decreasing trend, and a notable reduction in food intake was observed during the experiment. This could be associated with celastrol's potential to enhance leptin sensitivity, thereby suppressing appetite [36]. Conversely, the body weight of mice in the combination treatment group remained relatively stable, suggesting that the concurrent administration of celastrol and olaparib may mitigate the weight-reducing effect of celastrol to some extent. Additionally, the weights of the major organs in mice did not exhibit appreciable changes, indicating that the drug treatments did not manifest notable toxicity in normal organs (Fig. 5e, f). Moreover, IHC staining of Ki-67 was employed to assess proliferative activity within the PC3 xenograft tumors. The data demonstrated a significant reduction in Ki-67 protein expression following combination therapy ($P<0.01$) (Fig. 5g), indicative of decreased tumor cell proliferation. These collective findings imply that the combined regimen of

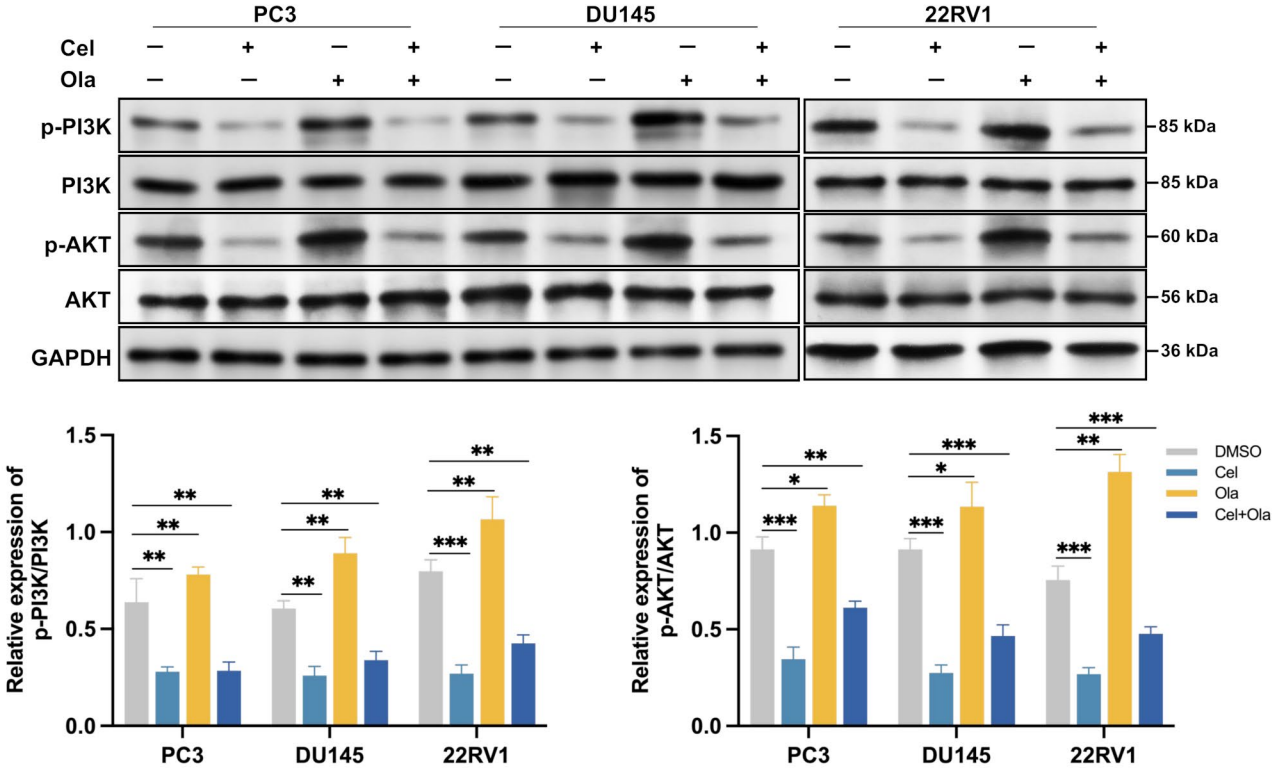

Fig. 4 Celastrol downregulates PI3K/AKT pathway and enhances sensitivity to olaparib. Western blot analysis of PI3K/AKT pathway modulation in PC3, DU145 and 22RV1 cells treated with celastrol (1 μM) and olaparib (50 μM), either agent alone, or DMSO, for 48 h. Shown are the means ± SD from 3 experiments (*$P<0.05$, **$P<0.01$, ***$P<0.001$)

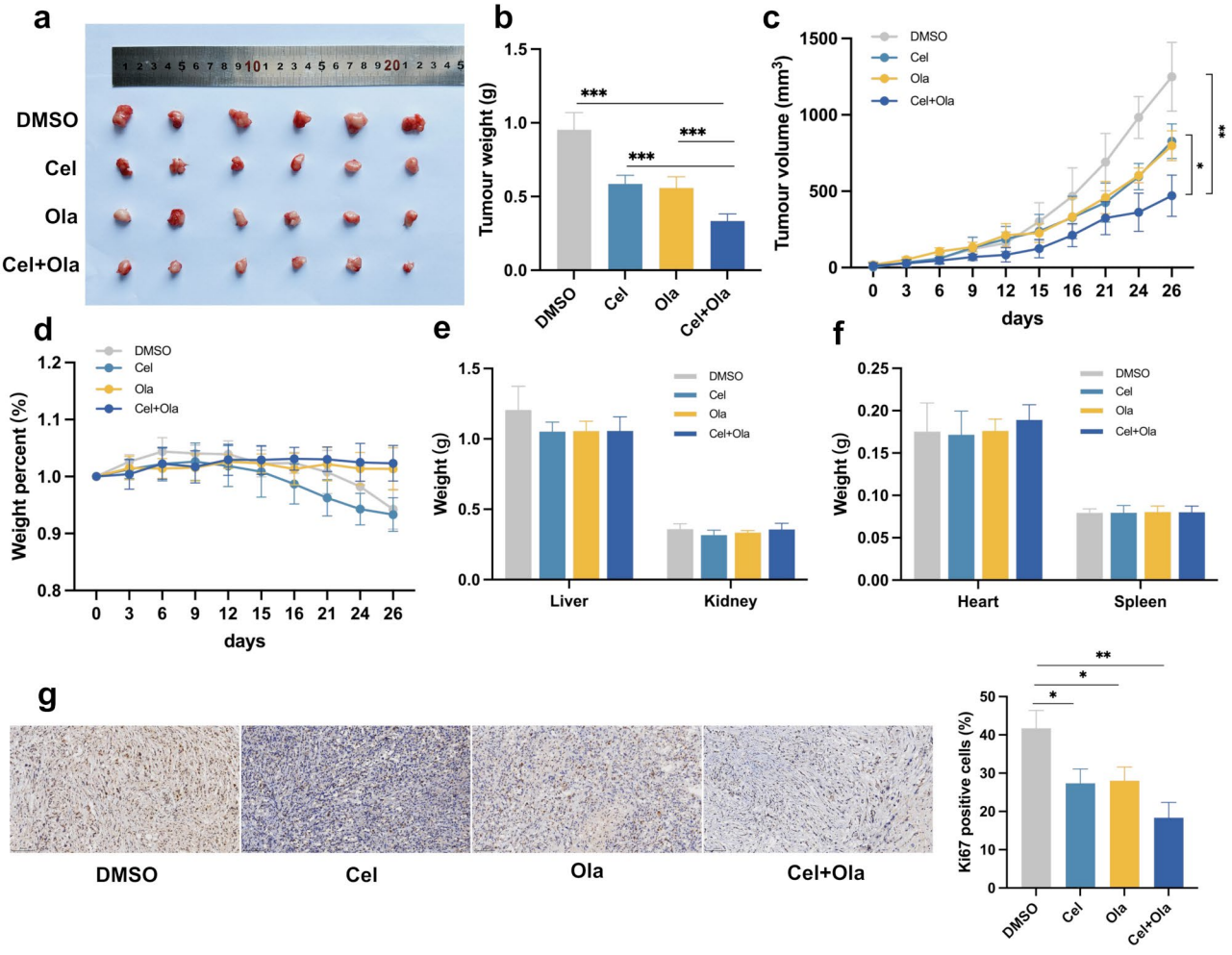

Fig. 5 Cleastrol combined with olaparib exhibits an enhanced anti-tumor effect in PC3 xenografts in vivo. (**a**) Representative images of PCa tumor xenografts from each mouse ($n = 6$/group). (**b**, **c**) The weight and volume of tumors from each experimental group were documented and subjected to analysis. (**d**) Body weight percent change in mice bearing PCa xenografts over 26 days. (**e**, **f**) The weights of principle organs were measured and analyzed after sacrifice. (**g**) IHC for Ki-67 was conducted on tumor tissue and quantified using Image software. Scale bars: 100 μm. Shown are the means ± SD from 3 experiments (*$P < 0.05$, **$P < 0.01$, ***$P < 0.001$)

celastrol and olaparib significantly hinders in vivo tumor growth in the PC3 xenograft setting.

Discussion

PCa is characterized by substantial genomic heterogeneity, originating from an accumulation of genetic and epigenetic alterations that drive carcinogenesis [2]. This diversity can be attributed to multiple factors, including dysregulated transcription in AR and PI3K signaling pathways, as well as defects in DNA repair mechanisms, all of which contribute significantly to the initiation and progression of PCa [34, 37, 38]. Thses present a significant challenge in the treatment of PCa. Olaparib, a PARP inhibitor, has garnered approval for treating metastatic breast cancer and mCRPC patients harboring genetic mutations in HRR genes [28, 39]. Clinical evidence has demonstrated significant benefits of olaparib in these patient populations; however, the development of drug resistance inevitably occurs during its clinical application. In cancer cells, the PI3K/AKT pathway may be activated as a survival mechanism in response to the DNA damage caused by olaparib. Therefore, combining olaparib with agents that can inhibit the PI3K/AKT pathway is a strategy that is being researched to overcome resistance and enhance the efficacy of olaparib in cancer therapy [40, 41].

In this study, we initially revealed the overexpression of HSP90AB1 and PARP1 across various cancer types, particularly in PCa. HSP90AB1, a member of the HSP90 family, functions as a molecular chaperone that is pivotal in maintaining cellular proteostasis [12]. Due to its integral role in protein homeostasis, HSP90AB1 is essential for supporting cells under stress conditions that are commonly encountered within the tumor microenvironment.

By stabilizing a wide range of oncoproteins, such as kinases, hormone receptors, and transcription factors, HSP90AB1 inadvertently promotes the malignant phenotype [19, 20]. HSP90AB1 is commonly overexpressed in a variety of cancers, with this upregulation typically linked to poor prognostic outcomes and increased resistance to standard chemotherapy and radiotherapy treatments [12, 42, 43]. Based on these findings, we hypothesized that inhibition of HSP90AB1 may enhance the sensitivity of PCa cells to olaparib.

Upon utilizing shRNA to interfere with HSP90AB1, we discovered that HSP90AB1 knockdown significantly augmented the inhibitory effect of olaparib on 22RV1, PC3 and DU145 cell viability. This suggested that HSP90AB1 potentially mediates the sensitivity of PCa cells to olaparib. Subsequently, we employed the HSP90AB1 inhibitor celastrol and the PARP inhibitor olaparib to conduct further experiments on relevant cellular phenotypes. Notably, the synergy between olaparib and celastrol, resulting in diminished clonogenic survival, migration, proliferation and viability of PCa cells, suggests that combining with celastrol enhances the anti-tumor effect of olaparib in vitro. Additionally, the enhanced accumulation of DNA damage upon treatment with both agents suggests that celastrol may amplify the DNA-damaging effects of olaparib, thereby intensifying its cytotoxicity against PCa cells.

The PI3K/AKT pathway, a crucial regulator of cell growth and survival, plays a significant role in both the development and therapy of PCa [34, 35]. In our study, we observed that olaparib induces the activation of AKT, as a response to cellular stressors, aligning with findings from previous research [44]. However, this phenomenon was attenuated when combined with celastrol. This suggested that celastrol's ability to downregulate the PI3K/AKT pathway provides further mechanistic insight into how this combination therapy hampers the survival of PCa cells. In vivo, the anti-tumor effects of the celastrol and olaparib combination were demonstrated in PC3 xenograft models, confirming the translational potential of our in vitro findings. The absence of significant weight loss or alterations in organ weights in the combination treatment group implies a favorable toxicity profile. Additionally, the expression of the tumor proliferation marker Ki-67 was significantly decreased in the group receiving the combination treatment.

Celastrol, a natural triterpenoid compound extracted from the roots of the Thunder God Vine (*Tripterygium wilfordii)*, has garnered considerable attention in recent years for its potential in cancer therapy. Known for its anti-inflammatory and antioxidant properties [22, 23], celastrol's mechanism of action in cancer treatment is multifaceted. It has been shown to induce apoptosis, inhibit angiogenesis, and suppress cell proliferation in various cancer cell lines. Celastrol has also been observed to sensitize cancer cells to conventional chemotherapeutic agents and radiotherapy, further enhancing its therapeutic potential.

The findings from our study revealed that the combined therapy of celastrol and olaparib exerted notably more potent inhibitory effects on the proliferation of PCa cells than either celastrol or olaparib when used as single agents, observable in both in vitro and in vivo settings. Highlighting the potential of combining celastrol with olaparib as a novel therapeutic strategy for PCa. This combination could address the limitations of PARP inhibitor monotherapy, particularly in cancers exhibiting inherent or acquired resistance.

Conclusions

Our research demonstrated that both HSP90AB1 and PARP1 exhibit high expression levels in PCa cells. Furthermore, we have discovered that the HSP90 inhibitor, celastrol, amplifies the anticancer efficacy of the PARP inhibitor, olaparib, both in vitro and *in vivo.* These insights pave the way for a promising therapeutic approach in PCa, focusing on the concurrent inhibition of HSP90AB1 and PARP1.

Abbreviations

PCa	Prostate cancer
HSP90AB1	Heat shock protein alpha family class B
PARP1	Poly (ADP-ribose) polymerase 1
DSB	Double strand breaks

Acknowledgements

No applicable.

Author contributions

Houqiang Xu conceived the project. Xiaoyan Ma prepared all the materials. Mengqiu Huang carried out the in vitro and in vivo experiments. All authors participated in the discussion and evaluation of experimental results. Mengqiu Huang completed the first draft and drew the schematic figures. Lin Chen finalized the manuscript.

Funding

The authors would like to acknowledge the financial support provided by the National Natural Science Foundation of China under Grant Number 31860242 and Zunyi City Science and Technology Plan Project [Zun City Science and Technology Cooperation HZ No. (2023) 248].

Data availability

No datasets were generated or analysed during the current study.

Declarations

Ethics approval and consent to participate

All animal experimental procedures conducted in this study were approved by the Laboratory Animal Ethics Committee of Guizhou University. The approval was granted under the license number EAE-GZU-2023-E025.

Consent for publication

Not applicable.

Competing interests

The authors declare no competing interests.

Received: 25 July 2024 / Accepted: 21 October 2024
Published online: 26 October 2024

References

1. Andriole GL, Crawford ED, Grubb Iii RL, Buys SS, Chia D, Church TR, Fouad MN, Gelmann EP, Kvale PA, Reding DJ. Mortality results from a randomized prostate-cancer screening trial[J]. N Engl J Med. 2009;360(13):1310–9.
2. Grasso CS, Wu Y-M, Robinson DR, Cao X, Dhanasekaran SM, Khan AP, Quist MJ, Jing X, Lonigro RJ, Brenner JC. The mutational landscape of lethal castration-resistant prostate cancer[J]. Nature. 2012;487(7406):239–43.
3. Pang B, Zhu Y, Ni J, Thompson J, Malouf D, Bucci J, Graham P, Li Y. Extracellular vesicles: the next generation of biomarkers for liquid biopsy-based prostate cancer diagnosis[J]. Theranostics. 2020;10(5):2309.
4. Bostwick DG, Burke HB, Djakiew D, Euling S, Ho SM, Landolph J, Morrison H, Sonawane B, Shifflett T, Waters DJ. Human prostate cancer risk factors[J]. Cancer: Interdisciplinary Int J Am Cancer Soc. 2004;101(S10):2371–490.
5. Gann PH. Risk factors for prostate cancer[J]. Rev Urol. 2002;4(Suppl 5):S3.
6. Kensler KH, Rebbeck TR. Cancer progress and priorities: prostate cancer[J]. Cancer Epidemiol Biomarkers Prev. 2020;29(2):267–77.
7. Loeb S, Bjurlin MA, Nicholson J, Tammela TL, Penson DF, Carter HB, Carroll P, Etzioni R. Overdiagnosis and overtreatment of prostate cancer[J]. Eur Urol. 2014;65(6):1046–55.
8. Cannata DH, Kirschenbaum A, Levine AC. Androgen deprivation therapy as primary treatment for prostate cancer[J]. J Clin Endocrinol Metabolism. 2012;97(2):360–5.
9. Nguyen PL, Alibhai SM, Basaria S, D'amico A V, Kantoff PW, Keating NL, Penson DF, Rosario DJ, Tombal B, Smith MR. Adverse effects of androgen deprivation therapy and strategies to mitigate them[J]. Eur Urol. 2015;67(5):825–36.
10. Crawford ED, Higano CS, Shore ND, Hussain M, Petrylak DP. Treating patients with metastatic castration resistant prostate cancer: a comprehensive review of available therapies[J]. J Urol. 2015;194(6):1537–47.
11. Schmidt KT, Huitema AD, Chau CH, Figg WD. Resistance to second-generation androgen receptor antagonists in prostate cancer[J]. Nat Reviews Urol. 2021;18(4):209–26.
12. Haase M, Fitze G. HSP90AB1: helping the good and the bad[J]. Gene. 2016;575(2):171–86.
13. Wang H, Deng G, Ai M, Xu Z, Mou T, Yu J, Liu H, Wang S, Li G. Hsp90ab1 stabilizes LRP5 to promote epithelial–mesenchymal transition via activating of AKT and Wnt/β-catenin signaling pathways in gastric cancer progression[J]. Oncogene. 2019;38(9):1489–507.
14. Lin T, Qiu Y, Peng W, Peng L. Heat shock protein 90 family isoforms as prognostic biomarkers and their correlations with immune infiltration in breast cancer[J]. BioMed Research International, 2020, 2020: 1–15.
15. Liu K, Kang M, Li J, Qin W, Wang R. Prognostic value of the mRNA expression of members of the HSP90 family in non–small cell lung cancer[J]. Experimental Therapeutic Med. 2019;17(4):2657–65.
16. Minghui W, Lin F, Ping L, Naijun H, Yanning G, Ting X. Hsp90AB1 protein is overexpressed in non-small cell lung cancer tissues and associated with poor prognosis in lung adenocarcinoma patients[J]. Zhongguo Fei Ai Za Zhi, 2016, 19(2).
17. Xiao H, Wang B, Xiong HX, Guan JF, Wang J, Tan T, Lin K, Zou SB, Hu ZG, Wang K. A novel prognostic index of hepatocellular carcinoma based on immunogenomic landscape analysis[J]. J Cell Physiol. 2021;236(4):2572–91.
18. Zhang H, Yin X, Zhang X, Zhou M, Xu W, Wei Z, Song C, Han S, Han W. HSP90AB1 promotes the proliferation, migration, and glycolysis of head and neck squamous cell carcinoma[J]. Technol Cancer Res Treat. 2022;21:15330338221118202.
19. Taipale M, Jarosz DF, Lindquist S. HSP90 at the hub of protein homeostasis: emerging mechanistic insights[J]. Nat Rev Mol Cell Biol. 2010;11(7):515–28.
20. Hoter A, El-Sabban ME, Naim HY. The HSP90 family: structure, regulation, function, and implications in health and disease[J]. Int J Mol Sci. 2018;19(9):2560.
21. Chadli A, Felts SJ, Wang Q, Sullivan WP, Botuyan MV, Fauq A, Ramirez-Alvarado M, Mer G. Celastrol inhibits Hsp90 chaperoning of steroid receptors by inducing fibrillization of the co-chaperone p23[J]. J Biol Chem. 2010;285(6):4224–31.
22. Allen SD, Liu Y-G, Kim T, Bobbala S, Yi S, Zhang X, Choi J, Scott EA. Celastrol-loaded PEG-b-PPS nanocarriers as an anti-inflammatory treatment for atherosclerosis[J]. Biomaterials Sci. 2019;7(2):657–68.
23. Allison AC, Cacabelos R, Lombardi VR, Álvarez XA, Vigo C. Celastrol, a potent antioxidant and anti-inflammatory drug, as a possible treatment for Alzheimer's disease[J]. Prog Neuropsychopharmacol Biol Psychiatry. 2001;25(7):1341–57.
24. Lim HY, Ong PS, Wang L, Goel A, Ding L, Wong A, L-A, Ho PC-L, Sethi G, Xiang X, Goh BC. Celastrol in cancer therapy: recent developments, challenges and prospects[J]. Cancer Lett. 2021;521:252–67.
25. Dziadkowiec KN, Gąsiorowska E, Nowak-Markwitz E, Jankowska A. PARP inhibitors: review of mechanisms of action and BRCA1/2 mutation targeting[J]. Menopause Review/Przegląd Menopauzalny. 2016;15(4):215–9.
26. Moore K, Colombo N, Scambia G, Kim B-G, Oaknin A, Friedlander M, Lisyanskaya A, Floquet A, Leary A, Sonke GS. Maintenance olaparib in patients with newly diagnosed advanced ovarian cancer[J]. N Engl J Med. 2018;379(26):2495–505.
27. Tutt AN, Garber JE, Kaufman B, Viale G, Fumagalli D, Rastogi P, Gelber RD, De Azambuja E, Fielding A, Balmaña J. Adjuvant olaparib for patients with BRCA1-or BRCA2-mutated breast cancer[J]. N Engl J Med. 2021;384(25):2394–405.
28. De Bono J, Mateo J, Fizazi K, Saad F, Shore N, Sandhu S, Chi KN, Sartor O, Agarwal N, Olmos D. Olaparib for metastatic castration-resistant prostate cancer[J]. N Engl J Med. 2020;382(22):2091–102.
29. Bochum S, Berger S, Martens UM. Olaparib[J] Small Molecules Oncol, 2018: 217–33.
30. Hussain M, Mateo J, Fizazi K, Saad F, Shore N, Sandhu S, Chi KN, Sartor O, Agarwal N, Olmos D. Survival with olaparib in metastatic castration-resistant prostate cancer[J]. N Engl J Med. 2020;383(24):2345–57.
31. Lim JS, Tan DS. Understanding resistance mechanisms and expanding the therapeutic utility of PARP inhibitors[J]. Cancers. 2017;9(8):109.
32. Rich T, Allen RL, Wyllie AH. Defying death after DNA damage[J]. Nature. 2000;407(6805):777–83.
33. Valdiglesias V, Giunta S, Fenech M, Neri M, Bonassi S. γH2AX as a marker of DNA double strand breaks and genomic instability in human population studies[J]. Mutat Research/Reviews Mutat Res. 2013;753(1):24–40.
34. Chen H, Zhou L, Wu X, Li R, Wen J, Sha J, Wen X. The PI3K/AKT pathway in the pathogenesis of prostate cancer[J]. Front Biosci (Landmark Ed). 2016;21(5):1084–91.
35. Sarker D, Reid AH, Yap TA, De Bono JS. Targeting the PI3K/AKT pathway for the treatment of prostate cancer[J]. Clin Cancer Res. 2009;15(15):4799–805.
36. Liu J, Lee J, Hernandez Ma, Mazitschek S, Ozcan R. Treatment of obesity with celastrol[J]. Cell. 2015;161(5):999–1011.
37. Culig Z, Santer FR. Androgen receptor signaling in prostate cancer[J]. Cancer Metastasis Rev. 2014;33:413–27.
38. Mateo J, Boysen G, Barbieri CE, Bryant HE, Castro E, Nelson PS, Olmos D, Pritchard CC, Rubin MA, De Bono JS. DNA repair in prostate cancer: biology and clinical implications[J]. Eur Urol. 2017;71(3):417–25.
39. Robson M, Im S-A, Senkus E, Xu B, Domchek SM, Masuda N, Delaloge S, Li W, Tung N, Armstrong A. Olaparib for metastatic breast cancer in patients with a germline BRCA mutation[J]. N Engl J Med. 2017;377(6):523–33.
40. Wang D, Wang M, Jiang N, Zhang Y, Bian X, Wang X, Roberts TM, Zhao JJ, Liu P, Cheng H. Effective use of PI3K inhibitor BKM120 and PARP inhibitor Olaparib to treat PIK3CA mutant ovarian cancer[J]. Oncotarget. 2016;7(11):13153.
41. Konstantinopoulos PA, Barry WT, Birrer M, Westin SN, Cadoo KA, Shapiro GI, Mayer EL, O'cearbhaill RE, Coleman RL, Kochupurakkal B. Olaparib and α-specific PI3K inhibitor alpelisib for patients with epithelial ovarian cancer: a dose-escalation and dose-expansion phase 1b trial[J]. Lancet Oncol. 2019;20(4):570–80.
42. Neckers L. Hsp90 inhibitors as novel cancer chemotherapeutic agents[J]. Trends Mol Med. 2002;8(4):S55–61.
43. Whitesell L, Lindquist SL. HSP90 and the chaperoning of cancer[J]. Nat Rev Cancer. 2005;5(10):761–72.
44. Tapodi A, Debreceni B, Hanto K, Bognar Z, Wittmann I, Gallyas F, Varbiro G, Sumegi B. Pivotal role of akt activation in mitochondrial protection and cell survival by poly (ADP-ribose) polymerase-1 inhibition in oxidative stress[J]. J Biol Chem. 2005;280(42):35767–75.

Publisher's note